Calculation of the surface tension from Monte Carlo simulations: Does the model impact on the finite-size effects?

F. Biscay,[1,2] A. Ghoufi,[1,a)] F. Goujon,[2] V. Lachet,[1] and P. Malfreyt[2,b)]
[1]*IFP, 1-4 Av. de Bois Préau, 92852 Rueil Malmaison Cedex, France*
[2]*Laboratoire de Thermodynamique et Interactions Moléculaires, FRE CNRS 3099, Université Blaise Pascal, 63177 Aubière Cedex, France*

(Received 24 February 2009; accepted 21 April 2009; published online 13 May 2009)

We report two-phase Monte Carlo simulations of the liquid-vapor interface of the Lennard-Jones (LJ) fluids in order to study the impact of the methodology used for the energy calculation on the oscillatory behavior of the surface tension with the system sizes. The surface tension values are illustrated through the LJ parameters of methane. The first methodology uses a standard truncated LJ potential, the second one adds a long range correction (LRC) contribution to the energy into the Metropolis scheme, and the third one uses a LJ potential modified by a polynomial function in order to remove the discontinuities at the cutoff distance. The surface tension is calculated from the mechanical and thermodynamic routes and the LRCs to the surface tension are systematically calculated from appropriate expressions within these definitions. The oscillatory behavior has been studied as a function of the size of the interfacial area and of the length of the dimension perpendicular to the surface. We show that the methodology has an important effect on the oscillatory variation in the surface tension with the system size. This oscillatory variation in the surface tension with the system size is investigated through its intrinsic and LRC contributions. We complete this work by studying the dependence of the surface tension with respect to the cutoff distance when the LRC part to the energy is considered into the Metropolis scheme.
 [DOI: 10.1063/1.3132708]

I. INTRODUCTION

The most straightforward method for the surface tension calculation with a molecular description of the interface consists of explicitly modeling the liquid-vapor interface by using a liquid-slab arrangement. This leads to heterogeneous systems where a nonuniformity of the density number takes place along the direction normal to the interface. These two-phase simulations require to pay special attention on a certain number of factors which can impact the results of surface tension: The size effects due to the number of particles and to the surface area,[1,2] the periodic boundary conditions,[1,3] the range of interactions,[4–7] the truncation effects involved in the calculation of the potential and the corresponding force,[4,8,9] the mechanical and thermodynamic definitions used for the surface tension calculation,[9–11] and the long range corrections (LRCs) to the surface tension.[6,8,9,11–13]

The surface tension (γ) can be calculated by using a certain number of operational expressions. The most general working expression uses macroscopic normal and tangential pressures which can be related to the derivative of the pair potential. The final form has been obtained by Kirkwood and Buff[14–17] (KB) and gives a macroscopic scalar surface tension. In the case of a planar liquid-vapor interface lying in the x,y plane, the density gradient takes place in the z direction normal to the surface. The surface tension can be expressed as $\int_{-\infty}^{\infty}(p_N(z)-p_T(z))dz$, where $p_N(z)$ and $p_T(z)$ are local values of the normal and tangential components of the pressure tensor, respectively. There are many ways of expressing the local components of the pressure which depend on the contour joining two interacting molecules. Irving and Kirkwood[18–21] (IK) use a straight line to join the two particles. This choice is the most natural and the one generally made. Nevertheless, the scalar value of surface tension is invariant to the choice of the contour. The test-area (TA) method based upon the perturbation formalism was proposed by Gloor *et al.*[10] for the calculation of the surface tension. This method takes advantage of expressing the surface tension as a difference in energy between a reference state and a perturbed state characterized by an infinitesimal increase or decrease in the surface. Until recently, only the method of IK was designed to provide a profile of the surface tension. A local description of the surface tension was missing within the TA method. This led us to establish in a previous work the local expression of the surface tension calculated from the TA approach.[9]

The use of truncated potentials in the Monte Carlo (MC) and molecular dynamics (MD) bulk simulations requires to add LRCs to the thermodynamic properties at the end of simulations by considering that the radial distribution function is unity for separation distance greater that the cutoff radius. However, when the liquid-vapor interface is explicitly taken into account, the system shows a nonuniform density

a)Present address: Institut de Physique de Rennes, UMR CNRS 6251, Université de Rennes I, 35042 Rennes Cedex, France
b)Author to whom correspondence should be addressed. Electronic mail: patrice.malfreyt@univ-bpclermont.fr.

profile along the normal to the surface. It means that the standard bulk LRCs cannot be applied to the thermodynamic properties. Several approaches have been developed for the treatment of these tail corrections in heterogeneous systems. The first approach consisted of performing standard molecular simulations using truncated potentials and correcting the thermodynamic properties by specific tail contributions at the end of the run.[22–24] The second more sophisticated approach consisted of adding the LRC contributions to the configurational energy during the course of the simulation and in applying appropriate LRC parts to the thermodynamic properties at the end.[12,13,25–27] The third approach avoids the use of LRCs during or at the end of the simulations by using the lattice sum method to model the dispersive interactions.[5] This approach aims to model the full Lennard-Jones (LJ) potential.

When the LRCs to the configurational energy are included on the fly at each step, different schemes have been proposed. Guo and Lu[12] suggested an approach based on the assumption of local dependence of the configurational energy. The energy of the system is then corrected by two terms: One relating directly to the density of the local slab and another is due to the density differences between the local slab k value and those around the slab k element. The authors proposed the operational expressions for the tail corrections to the pressure, surface tension, and chemical potential. Mecke *et al.*[26] included the LRCs within MD simulation by including an additive force contribution in the direction perpendicular to the interface. They also proposed an operational expression for correcting the surface tension at the end of the simulation. The LRC values of the surface tensions calculated from these two approaches were compared on the surface tension of n-alkanes and were found very close within the standard deviations.[6] The tail correction scheme of Janecek[27] differs from that of Mecke *et al.* in that it takes into account particle-slab interactions arising from fluid slabs that are within a longitudinal cutoff distance of a given particle. Within this scheme, the energy and force expressions were established indicating that this scheme can be used with MC and MD simulations. A recent study[13] tends to show that the surface tension becomes cutoff independent when this scheme of tail correction is used.[13]

An alternative to the use of the LRCs consists of modeling the full potential. The dispersion term of the LJ potential is then calculated with a lattice sum method[5] in a way similar to that used for the calculation of the electrostatic interactions with the Ewald summation method. This method is not easily applicable to molecular systems for which the force fields have been established from MC or MD simulations using the standard LJ potential for the modeling of the intramolecular and intermolecular interactions. Additionally, this way of calculating the intermolecular interactions represents a significant computational cost.[13]

An indirect route based upon the free energy methods allows the calculation of the surface tension without the physical presence of the interface. Such method avoids the use of LRCs for heterogeneous systems. The grand canonical transition matrix Monte Carlo (GC-TMMC)[28,29] method determines the density dependence of the free energy of a fluid at a given temperature. When the GC-TMMC method is associated with the Binder's approach,[30] the surface tension is related to the free energy barrier between vapor and liquid phases, which is calculated from a GC-TMMC probability distribution.[31–34] Within the Binder's approach, the density dependence of the system can be explored with the aid of histogram reweighting method.[35,36] This approach has been combined with the finite-size scaling (FSS) to give surface tensions on LJ,[13,28,31] square well,[32] n-alkanes,[33] and LJ mixtures.[37] A comparison between the FSS/GC-TMMC method and the two-phase method has been carried out recently.[13]

In this paper, we only focus on the MC simulation of a two-phase system where inconsistent treatment of the LRCs to the surface tension can lead to conflicting results between the different methods. It is essential to associate an appropriate expression of the tail correction consistent with that of the intrinsic part of the surface tension. A certain number of expressions for calculating the LRC contributions of the surface tensions have been developed.[12,22,23,25,26,38] Some of them[12,25,26,38] express the LRC contributions of the surface tension along the direction normal to the interface. Our conclusions from previous works[9,11,39–42] showed that the different methods (IK, TA, and KB) match very well as long as appropriate LRC contributions are included in the calculation. It is now well established that the LRCs of the surface tension can represent up to 30% of the total value for cutoff radii similar to those used for homogeneous systems. The surface tension calculation[9] is also sensitive to the truncation of the potential since some definitions as IK and KB use the derivative of the potential, whereas others as TA use the configurational energy.

Recent papers[1,43] have shown that the two-phase simulation method leads to an oscillatory behavior of the surface tension with respect to the interfacial area. The authors have correlated these oscillations to the combined use of periodic boundary conditions and small interfacial areas. The combination of these two factors introduces an artificial oscillatory anisotropy[1,3] in the pressure tensor that makes γ dependent on the surface area. This finite-size effect of surface area on surface tension has also been observed in other types of approaches.[2,28,31]

We have calculated the surface tension of the liquid-vapor interface of water,[11,39] acid gases,[39,40] linear and branched alkanes,[41] and cyclic and aromatic hydrocarbons[42] from MC simulations. In these calculations, we did not find any oscillatory behavior of the surface tension with respect to the surface area for the range of interfacial areas studied. These MC simulations incorporated the LRC to the configurational energy on the fly. The tail correction to the configurational energy was calculated from the scheme of Guo and Lu.[12] These results lead us to address the following fundamental questions:

- Do the finite-size effects similarly impact on the surface tension when the LRC part to the energy is included during the course of the simulation?

- Does the oscillatory effect of the surface tension depend on the definition (KB, IK, and TA) used for the calculation of the surface tension?
- How do the finite-size effects affect the intrinsic and LRC part of the surface tension?
- Does the oscillation of the surface tension with respect to box dimensions depend on the way the interactions are truncated?
- Are the surface tension and its LRCs really dependent on the cutoff value when the LRC part to the energy is added on the fly?
- Is there an oscillatory effect of the surface tension as a function of the size of the simulation box in the direction normal to the surface?

To address these questions, we propose to perform MC simulations on the liquid-vapor interface of the LJ fluid at a reduced temperature of 0.8. To compare the results of surface tensions with those carried out on the liquid-vapor interfaces of alkanes, we use the LJ parameters of methane. These simulations are carried out using three different potentials: A truncated LJ potential, a truncated LJ potential corrected by the addition of a LRC term, and a LJ potential modified by a spline function in order to remove the discontinuities in the force and energy equations. The surface tension is calculated through the mechanical route using the KB and IK expressions and through the thermodynamic route using the TA approach. The simulations are performed for different surface areas at a fixed value of L_z and for different values of L_z at a fixed surface area. Different simulations are carried out to investigate the dependence of the intrinsic and LRC contributions to the surface tension with respect to the cutoff radius.

The outline of this paper is as follows. In Sec. II, we present the different potentials used and the scheme of Guo and Lu for the correction of the configurational energy. Section III presents the KB, IK, and TA operational expressions of the surface tension together with those of the corresponding LRC part. The results and discussions are provided in Sec. IV. The main conclusions of this work are summarized in Sec. V.

II. SIMULATION METHODOLOGY

A. Potential model

The LJ methane particle is modeled using a united-atom description with the parameters proposed by Möller and Oprzynski.[44] The molecules interact through a LJ potential

$$u_{\mathrm{LJ}} = 4\epsilon_{ij}\left[\left(\frac{\sigma_{ij}}{r_{ij}}\right)^{12} - \left(\frac{\sigma_{ij}}{r_{ij}}\right)^{6}\right], \tag{1}$$

where r_{ij} is the distance between molecules i and j. The LJ parameters σ_{ij} and ϵ_{ij}/k_B are 3.7327 Å and 149.92 K, respectively, where k_B is the Boltzmann constant. The simulations are performed using three different ways of applying the LJ potential. The first way is the most commonly applied in molecular simulation. It consists of truncating the potential at the cutoff radius (r_c) and is referred to as U_T in this paper,

$$U_T = \sum_{i=1}^{N-1}\sum_{j=i+1}^{N} u_T(r_{ij}), \tag{2}$$

where $u_T(r_{ij})$ is defined by

$$u_T(r_{ij}) = \begin{cases} u_{\mathrm{LJ}}(r_{ij}) & r_{ij} < r_c \\ 0 & r_{ij} \geq r_c \end{cases}. \tag{3}$$

In the second way, the potential used noted as U_{TLRC} is composed of both the truncated LJ potential and a term accounting for the LRCs U_{LRC} to the configurational energy

$$U_{\mathrm{TLRC}} = \sum_{i=1}^{N-1}\sum_{j=i+1}^{N} u_T(r_{ij}) + U_{\mathrm{LRC}}. \tag{4}$$

The LRC expressions to the configurational energy are given in Sec. II B for completeness.

In the third approach, the potential used noted as U_{SP} for spline potential corresponds to the standard truncated LJ potential changed by the addition of a polynomial function defined in Eq. (6),

$$U_{\mathrm{SP}} = \sum_{i=1}^{N-1}\sum_{j=i+1}^{N} u_{\mathrm{SP}}(r_{ij}), \tag{5}$$

with

$$u_{\mathrm{SP}}(r_{ij}) = \begin{cases} u_{\mathrm{LJ}}(r_{ij}) - u_{\mathrm{LJ}}(r_s) + a & r_{ij} < r_s \\ -\frac{b}{3}(r_{ij}-r_c)^3 - \frac{c}{4}(r_{ij}-r_c)^4 & r_s \leq r_{ij} < r_c \\ 0 & r_{ij} \geq r_c \end{cases}, \tag{6}$$

where the parameters a, b, and c are calculated by requiring that the first and second derivatives of the U_{SP} potential must be continuous at r_s and r_c. They are given by the following expressions:

$$\begin{aligned} c &= +\frac{\frac{\partial^2 u_{\mathrm{LJ}}}{\partial r_{ij}^2}(r_s)}{(r_s-r_c)^2} - 2\frac{\frac{\partial u_{\mathrm{LJ}}}{\partial r_{ij}}(r_c)}{(r_s-r_c)^3}, \\ b &= -\frac{\frac{\partial^2 u_{\mathrm{LJ}}}{\partial r_{ij}^2}(r_s)}{(r_s-r_c)} + 3\frac{\frac{\partial u_{\mathrm{LJ}}}{\partial r_{ij}}(r_s)}{(r_s-r_c)^2}, \\ a &= -\frac{b}{3}(r_s-r_c)^3 - \frac{c}{4}(r_s-r_c)^4. \end{aligned} \tag{7}$$

To compare the results with previous MC simulations of the LJ fluids,[1,2,4,13] we used $r_c = 9.3$ Å $= 2.5\sigma$ and $r_s = 8.3$ Å $= 2.2\sigma$.

B. Long range corrections to the energy

As the geometry of the system shows a heterogeneity along the axis normal to the interface (z-axis), we calculated the LRC to the repulsion-dispersion energy as a function of z_k by splitting the cell into slabs of width δz. The total LRC

TABLE I. Interfacial areas and L_z box dimensions given in angstroms and in reduced units of σ for each type of simulation. The numbers of methane molecules are also given for each set of parameters.

Constant L_z (L_z=242 Å=64.8σ)			Constant $A=L_xL_y$ ($L_x=L_y$=46 Å=12.3σ)		
L_x (Å)	L_x (σ)	N	L_z (Å)	L_z (σ)	N
20.0	5.4	250	157.7	42.2	250
23.0	6.2	375	161.5	43.3	375
25.0	6.7	500	165.3	44.3	500
27.0	7.2	625	169.2	45.3	625
29.0	7.8	750	173.0	46.3	750
30.0	8.0	875	176.8	47.4	875
32.0	8.6	1000	180.6	48.4	1000
36.5	9.8	1500	196.0	52.5	1500
40.0	10.7	2000	211.3	56.6	2000
43.5	11.7	2500	226.6	60.7	2500
46.0	12.3	3000	242.0	64.8	3000

energy U_{LRC} was then calculated by summing up all of the local contributions of each slab. The U_{LRC} term was then added to the total energy of the system to be used in the Metropolis scheme. The LRCs to the total energy within each kth slab are defined by two parts,[12]

$$U_{\mathrm{LRC}} = \sum_{k=1}^{N_z} u_{\mathrm{LRC}}(z_k) = \sum_{k=1}^{N_z} (u_{\mathrm{LRC}}^{(1)}(z_k) + u_{\mathrm{LRC}}^{(2)}(z_k)), \tag{8}$$

where N_z is the number of slabs and

$$u_{\mathrm{LRC}}^{(1)}(z_k) = \frac{8\pi}{3}\rho(z_k)^2 V_s \epsilon_{ij}\left[1/3\left(\frac{\sigma_{ij}^{12}}{r_c^9}\right) - \left(\frac{\sigma_{ij}^{6}}{r_c^3}\right)\right], \tag{9}$$

$$u_{\mathrm{LRC}}^{(2)}(z_k) = \pi\rho(z_k)V_s \int_{r_c}^{\infty} dr \int_{-r}^{r} d\Delta z \sum_{i=1}^{N_s} [\rho(z_{k+i}) - \rho(z_{k+i-1})] r u_{\mathrm{LJ}}(r). \tag{10}$$

$\rho(z_k)$ and V_s are respectively the density and the volume of the slab k. Δz is defined as the difference, $z-z_k$. N_s is the number of slabs between z and z_k. The first part of the long range contribution has an analytical form identical to the one associated with a homogeneous system but uses the local density $\rho(z_k)$ of the slab. The second part consists of a double integral which contains a series of density differences which render this part cumbersome to calculate. It has been shown[6,12] that this second part of the LRCs to the total configurational energy represents only a minor contribution to the total long range energy. This LRC energy U_{LRC} was updated after each move of molecular position.

C. Computational procedures

The simulation box was a rectangular parallelepipedic box of dimensions $L_xL_yL_z$ ($L_x=L_y$) with N methane molecules. The periodic boundary conditions were applied in the three directions. MC simulations were performed in the constant-NVT ensemble. All simulations were organized in cycles. Each cycle consisted of N translations of the methane molecules. The initial configuration was built by placing N molecules on nodes of a fcc centered orthorhombic lattice included in a cubic box. The number of molecules N and the initial volume were chosen in order to build a dense phase. The nodes of the lattice were randomly chosen. MC simulations in the NpT ensemble were first performed on this bulk monophasic fluid configuration. The dimension of the resulting box was increased along the z axis by placing two empty cells on both sides of the bulk liquid box. A typical MC run consisted of 200 000 cycles for equilibration and 200 000 cycles for the production phase.

The thermodynamic properties were calculated every 10 cycles leading to the storage of 20 000 configurations. The statistical errors for these properties were estimated using four superblock averages.

The MC calculations were carried out at T=120 K, which corresponds to a reduced temperature k_BT/ϵ equal to 0.8. The simulations were performed for different surface areas ranging from 20×20 to 46×46 Å^2 at a fixed value of L_z (242 Å) and for different L_z values varying from 157 to 242 Å at a fixed interfacial area of 46×46 Å^2 (see Table I for further details). The total number of molecules and the values of the L_x and L_z dimensions in units of σ are given in Table I.

III. CALCULATION OF THE SURFACE TENSION

The most commonly used methods[10,14,18–21] for the surface tension calculation are based upon the mechanical route and use of the tensorial components of the pressure. The first explicit form expresses the components of the pressure tensor as a function of the derivative of the intermolecular potential. This operational expression was given by KB (Ref. 14) and is referred here as the KB expression (γ_{KB}). The definition of IK (Ref. 19) (γ_{IK}) is based upon the notion of the force across a unit area and takes advantage of expressing the local components of the pressure tensor along the direction normal to the surface. A novel method based upon the thermodynamic definition of the surface tension (γ_{TA}) has been recently established by Gloor *et al.*[10] and consists of virtually changing the cross-sectional area of the system containing the interface. In what follows, we present the different operational expressions of the surface tension with the corresponding expressions of their LRCs.

Let us consider a system of N molecules with two planar liquid-vapor surfaces lying in the x,y plane, where z represents the direction normal to the surface.

A. Kirkwood–Buff relation

The molecular surface tension γ_{KB} was first introduced by KB (Ref. 14) and makes use of the molecular virial expression to give the following relationship:

$$\gamma_{KB} = \frac{1}{2A}\left\langle \sum_{i=1}^{N-1}\sum_{j=i+1}^{N} \frac{\mathbf{r_{ij}}\cdot\mathbf{r_{ij}} - 3z_{ij}\cdot z_{ij}}{2r_{ij}}\frac{du(r_{ij})}{dr_{ij}} \right\rangle, \tag{11}$$

where u is the potential described by either u_T or u_{SP}.

Specific LRCs were developed by Blokhuis *et al.*[23] and are based upon the approximations that the radial distribution function is equal to unity for r greater than the cutoff radius and that the density profile can be fitted to a hyperbolic function. This LRC expression takes the following form:

$$\gamma_{KB,LRC} = \frac{\pi}{2}(\rho_l - \rho_v)^2 \int_0^1 ds \int_{r_c}^{+\infty} dr \coth\left(\frac{2rs}{d}\right) \times \frac{du_{LJ}(r)}{dr} r^4(3s^3 - s), \tag{12}$$

where d is an estimation of the thickness of the interface and s is a parameter defined by $s=(z_i-z_j)/r_{ij}$.

B. Irving and Kirkwood definition

The method of IK (Ref. 19) expresses the surface tension from the local components of the pressure tensor

$$\gamma_{IK} = \frac{1}{2}\int_{-L_z/2}^{L_z/2} (p_N(z_k) - p_T(z_k))dz, \tag{13}$$

where $p_N(z_k)$ and $p_T(z_k)$ are the normal and tangential components of the pressure tensor along the normal to the surface, respectively. The method of IK (Ref. 19) is based upon the notion of the force across a unit area. The pressure tensor is then written as a sum of a kinetic term and a configurational term resulting from the intermolecular forces. Whereas the first term is well defined, the potential term is subjected to arbitrariness because there is no unique way to determine which intermolecular forces contribute to the stress across dA. There are many ways of choosing the contour joining two interacting particles. IK (Ref. 19) chose the straight line between the two particles. Other choices are possible and result from the lack of uniqueness in the definition of the microscopic stress tensor. The components of the pressure tensor[18,20,21] in the IK definition are expressed by

$$p_{\alpha\beta}(z_k) = \langle\rho(z_k)\rangle k_B T\mathbf{I} + \frac{1}{A} \times \left\langle \sum_{i=1}^{N-1}\sum_{j=i+1}^{N} (\mathbf{r_{ij}})_\alpha (\mathbf{F_{ij}})_\beta \frac{1}{|z_{ij}|}\theta\left(\frac{z_k - z_i}{z_{ij}}\right)\theta\left(\frac{z_j - z_k}{z_{ij}}\right)\right\rangle, \tag{14}$$

where $\mathbf{I}$ is the unit tensor and T is the input temperature. α and β represent x, y, or z direction. $\theta(x)$ is the unit step function defined by $\theta(x)=0$ when $x<0$ and $\theta(x)=1$ when $x\geq 0$. A is the surface area normal to the z axis. The distance z_{ij} between two molecular centers of mass is divided into N_s slabs of thickness δz. Following IK, the molecules i and j give a local contribution to the pressure tensor in a given slab if the line joining the centers of mass of molecules i and j crosses, starts, or finishes in the slab. Each slab has $1/N_s$ of the total contribution from the $i-j$ interaction. The normal component $p_N(z_k)$ is equal to $p_{zz}(z_k)$, whereas the tangential component is given by $\frac{1}{2}(p_{xx}(z_k)+p_{yy}(z_k))$. $\mathbf{F_{ij}}$ is the intermolecular force between molecules i and j and is expressed as

$$\mathbf{F_{ij}} = -\frac{\mathbf{r_{ij}}}{r_{ij}}\frac{du(r_{ij})}{dr_{ij}}, \tag{15}$$

where the derivative of the potential with respect to the distance is expressed by

$$\frac{dU(r_{ij})}{dr_{ij}} = \begin{cases} \dfrac{\partial u_{LJ}}{\partial r_{ij}} & r_{ij} < r_c \\ 0 & r_{ij} \geq r_c \end{cases} \tag{16}$$

with the simulations using the truncated potentials U_T and U_{TLRC}. The simulations done with the LJ potential changed by a spline function use the derivative expressed as

$$\frac{du(r_{ij})}{dr_{ij}} = \begin{cases} \dfrac{\partial u_{LJ}}{\partial r_{ij}} & r_{ij} < r_s \\ -b(r_{ij}-r_c)^2 - c(r_{ij}-r_c)^3 & r_s \leq r_{ij} < r_c \\ 0 & r_{ij} \geq r_c \end{cases}. \tag{17}$$

The appropriate LRC to IK definition of the normal and tangential components of the pressure tensor has been derived by Guo and Lu[12] and is composed of two parts as expressed in Eqs. (18) and (19),

$$\begin{aligned} p_{N,LRC}(z_k) &= p^{(1)}_{N,LRC}(z_k) + p^{(2)}_{N,LRC}(z_k) \\ &= -\frac{2\pi}{3}\rho^2(z_k)\int_{r_c}^{\infty} dr r^3 \frac{du_{LJ}(r)}{dr} \\ &\quad - \pi\rho(z_k)\int_{r_c}^{\infty} dr \int_{-r}^{r} d\Delta z[\rho(z) \\ &\quad - \rho(z_k)]\frac{du_{LJ}(r)}{dr}(\Delta z)^2. \end{aligned} \tag{18}$$

As concerns the tangential pressure, the first term is identical to the first term of the normal component, whereas the second term is expressed by

$$\begin{aligned} p^{(2)}_{T,LRC}(z_k) &= -\frac{\pi}{2}\rho(z_k)\int_{r_c}^{\infty} dr \int_{-r}^{r} d\Delta z[\rho(z) \\ &\quad - \rho(z_k)]\frac{du_{LJ}(r)}{dr}[r^2 - (\Delta z)^2]. \end{aligned} \tag{19}$$

The first term of $p_{N,LRC}(z_k)$ and $p_{T,LRC}(z_k)$ is identical to that used in homogeneous molecular simulations by using a local density $\rho(z_k)$ instead of a scalar density ρ, whereas the second term takes into account the density differences be-

tween the slabs. From these LRC expressions, it is then possible to calculate the LRC part of the surface tension. The operational expression of this LRC part of the surface tension[12] within the IK formalism is then given by

$$\gamma_{\mathrm{IK,LRC}}(z_k) = \frac{\pi}{2}\rho(z_k)\frac{V_s}{A}\int_{r_c}^{\infty} dr \int_{-r}^{r} d\Delta z \sum_{i=1}^{N_s} [\rho(z_{k+i}) - \rho(z_{k+i-1})]\frac{du_{\mathrm{LJ}}(r)}{dr}[r^2 - 3(\Delta z)^2]. \tag{20}$$

The total LRC to the surface tension is obtained by summing up the local contributions of each bin and dividing the result by 2.

C. Test-area method

The TA method[10] is based upon a thermodynamic route and expresses the surface tension as a change in the free energy[45] for an infinitesimal change in the surface area in the constant-*NVT* ensemble. This method used a perturbation process for which the perturbed system (state $^{A+\Delta A}$) is obtained from an infinitesimal change ΔA in the area A of the reference system. The box dimensions $(L_x^{(A+\Delta A)}, L_y^{(A+\Delta A)}, L_z^{(A+\Delta A)})$ in the perturbed system are obtained using the following transformations: $L_x^{(A+\Delta A)} = L_x^{(A)}\sqrt{1+\xi}$, $L_y^{(A+\Delta A)} = L_y^{(A)}\sqrt{1+\xi}$, $L_z^{(A+\Delta A)} = L_z^{(A)}/(1+\xi)$, where $\xi \ll 1$. The area $(A+\Delta A)$ of the perturbed state thus equals to $L_x^{(A)}L_y^{(A)}(1+\xi)$ and ΔA is equal to $L_x^{(A)}L_y^{(A)}\xi$. These transformations conserve the volume of the box in the perturbed state. This means that it is possible to express the surface tension as a ratio of partition function between the perturbed and reference states. $U^{(A)}(\mathbf{r}^N)$ and $U^{(A+\Delta A)}(\mathbf{r}'^N)$ are the configurational energies of the systems with an area A and a configurational space $\mathbf{r}^N$ and an area $A+\Delta A$ and a configurational space $\mathbf{r}'^N$, respectively. The transformations used in the perturbation process lead to the following equality: $d\mathbf{r}'^N = d\mathbf{r}^N$. This expression is the key to writing the surface tension as the average of $\exp(-\Delta U/kT)$ in the constant-*NVT* ensemble

$$\begin{aligned}\gamma_{\mathrm{TA}} &= \left(\frac{\partial F}{\partial A}\right)_{N,V,T} \\ &= \lim_{\xi\to 0} -\frac{k_BT}{\Delta A}\ln\left\langle \exp\left(-\frac{(U^{(A+\Delta A)}(\mathbf{r}'^N) - U^{(A)}(\mathbf{r}^N))}{k_BT}\right)\right\rangle_0 \\ &= \sum_k \lim_{\xi\to 0} -\frac{k_BT}{\Delta A}\ln \\ &\quad \times\left\langle \exp\left(-\frac{(U^{(A+\Delta A)}(z_k,\mathbf{r}'^N) - U^{(A)}(z_k,\mathbf{r}^N))}{k_BT}\right)\right\rangle_{k,A},\end{aligned} \tag{21}$$

where $\langle\cdots\rangle_{k,A}$ indicates that the average is carried out over the reference state and the k slabs. $U^{(A+\Delta A)}(z_k,\mathbf{r}'^N)$ and $U^{(A)}\times(z_k,\mathbf{r}^N)$ are the configurational energy of the slab k in the perturbed and reference states. The ambiguity[18] focuses on the part of the interaction energy to be included in the volume V_s of the slab. We adopt the definition of Ladd and Woodcock[46] and choose to assign in the slab centered on z_k two energy contributions: One contribution due to the energy between the molecules within the slab and a second contribution due to the energy of the molecules within the slab with those outside the slab. The energy of the slab at the position z_k is defined as

$$U_{z_k} = \frac{1}{2}\sum_{i=1}^{N}\sum_{j\neq i}^{N} H_k(z_i)u(r_{ij}), \tag{22}$$

where u represents u_{LJ} or u_{SP}. $H_k(z_i)$ is a top-hat function with functional values of

$$\begin{cases} H_k(z_i) = 1 & \text{for } z_k - \dfrac{\delta z}{2} < z_i < z_k + \dfrac{\delta z}{2} \\ H_k(z_i) = 0 & \text{otherwise} \end{cases}, \tag{23}$$

Using this definition, we respect the following condition:

$$\int_V dz_k U_{z_k} = U, \tag{24}$$

where U is the total configurational energy of the simulation box and V is the volume.

As concerns the LRC part to the surface tension calculated from the TA method, the total LRC contribution is expressed as a function of the total LRC energy U_{LRC} [see Eq. (25)]. We have already shown[9] that the difference between $u_{\mathrm{LRC}}^{(1),(A+\Delta A)}(z_k')$ and $u_{\mathrm{LRC}}^{(1),(A)}(z_k)$ vanishes because the transformation conserves the volume. Thus, the total value of the tail correction of the surface tension within the TA formalism is given by

$$\begin{aligned}\gamma_{\mathrm{TA,LRC}} &= \lim_{\xi\to 0} -\frac{k_BT}{\Delta A_\xi}\ln\left\langle \exp\left(-\frac{(U_{\mathrm{LRC}}^{(A+\Delta A)} - U_{\mathrm{LRC}}^{(A)})}{k_BT}\right)\right\rangle_0 \\ &= \sum_k^{N_s} \lim_{\xi\to 0} -\frac{k_BT}{\Delta A_\xi}\ln \\ &\quad \times\left\langle \exp\left(-\frac{(u_{\mathrm{LRC}}^{(2),(A+\Delta A)}(z_k')) - (u_{\mathrm{LRC}}^{(2),(A)}(z_k))}{k_BT}\right)\right\rangle_0 \\ &= \sum_k^{N_s} \gamma_{\mathrm{LRC}}(z_k).\end{aligned} \tag{25}$$

The calculation of the surface tension was carried out in the direct $(\gamma_{\mathrm{TA},D})$ and reverse $(\gamma_{\mathrm{TA},I})$ directions and was averaged over the two directions as $(\gamma_{\mathrm{TA},D} - \gamma_{\mathrm{TA},I})/2$. The calculation of the direct direction involves an increase in the surface area $(A+\Delta A)$, whereas a decrease in the surface area $(A-\Delta A)$ is performed in the reverse path. The ensemble average was carried out over the configurations of the reference system, whereas the configurations of the perturbed system did not participate to the Markov chain of states. The calculation can depend on the ξ parameter.[39,41,42] This value should be small enough to allow an accurate calculation of the surface tension from Eq. (21) and large enough to provide reasonable statistics for the Boltzmann factor. We found[9,39,41,42] that 5×10^{-4} was a good value for ξ for the calculation of the surface tension within the TA approach.

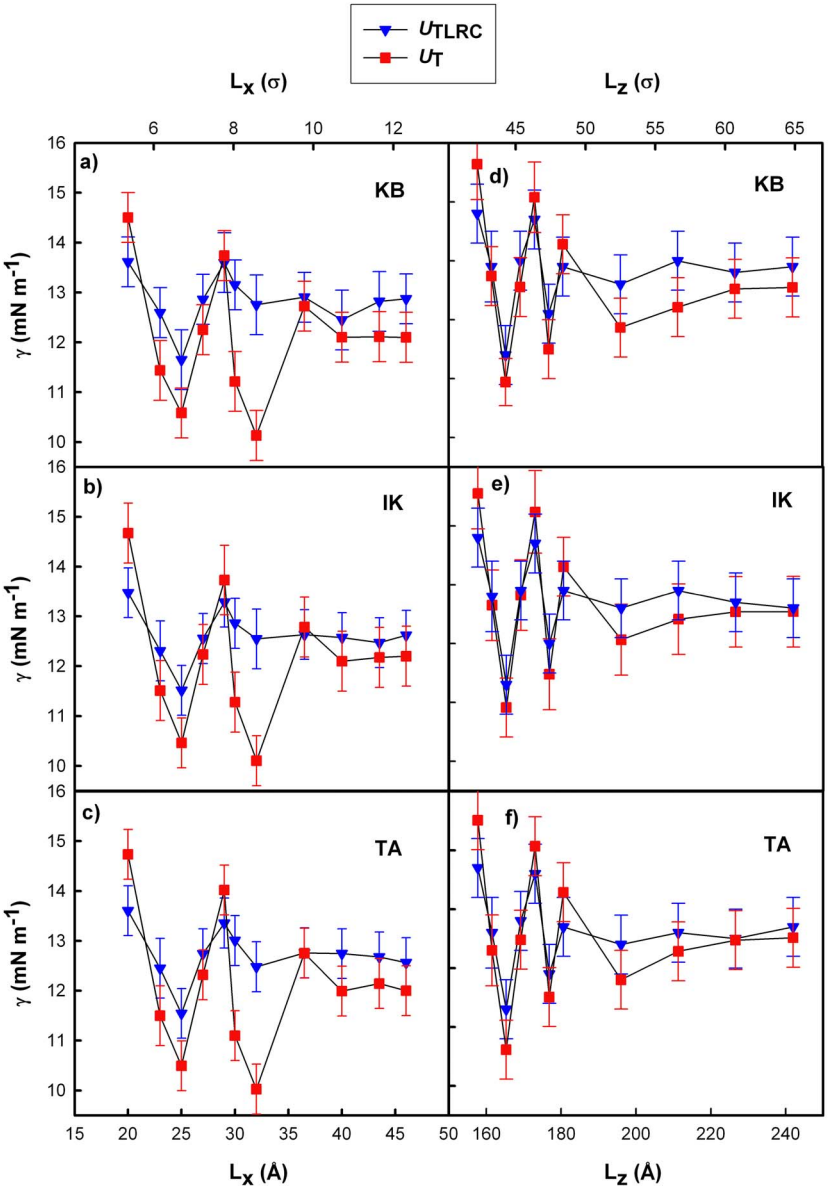

FIG. 1. (Color online) Total surface tension values (mN m^{-1}) calculated with respect to the L_x and L_z dimensions from MC simulations using the U_{TLRC} and U_T potentials. The bottom x axis is labeled in angstroms and the top x axis in units of σ. The surface tension is calculated from the virial route (KB and IK) and from the thermodynamic route (TA) as indicated in the different curves.

IV. RESULTS

Figures 1(a)–1(c) show the total values of the surface tension calculated from the KB, IK, and TA methods as a function of the L_x dimension for U_{TLRC} and U_T. For comparison with previous works, the L_x dimension is given in units of σ (top x axis) and in angstroms (bottom x axis). These figures support the fact that the surface tension is dependent on the interfacial area with an oscillatory behavior. The period of the oscillations is slightly smaller than 2σ in all cases. The value of the oscillation period is slightly higher than that found in the works of Orea *et al.*[1] and Errington and Kofke.[2] Interestingly, we observe that once the LRC contributions are considered within the Metropolis scheme, this oscillatory behavior of γ with the surface area is damped. The convergence of γ is obtained for smaller values of the interfacial area. The nearly constant value of γ with respect to L_x is reached for $L_x=9\sigma$ with U_{TLRC} and for $L_x=11\sigma$ with U_T. Additionally, one peak of oscillation is avoided with U_{TLRC} and the amplitude of the oscillations is also reduced. In fact, the difference between the smallest and largest value of γ along the oscillation curves calculated with U_T can represent up to 30% of γ, whereas this value decreases to 8% when the simulations are performed with U_{TLRC}. In order to avoid finite-size effects of γ related to the interfacial area, simulation boxes with a surface larger than $9\times 9\sigma^2$ are recommended. The damping of the oscillations with U_{TLRC} is observed for both the mechanical and the thermodynamic definitions of γ and is not dependent on the definition used.

Parts (d), (e), and (f) of Fig. 1 show the dependence of the surface tension with respect to the L_z dimension. The area of the interface was taken to $12.3\times 12.3\sigma^2$ in order to avoid the finite-size effects due to too small surface areas. The results tend to show that the incorporation of the LRC part into the configurational energy does not decrease significantly the first two oscillations but avoids a third peak of oscillation. Again, the convergence of γ with respect to L_z is reached for smaller L_z values with the use of U_{TLRC}. This dependence of γ with L_z is found whatever is the method employed (KB, IK, and TA). A L_z value of 50σ should be used with the U_{TLRC} potential to avoid a significant depen-

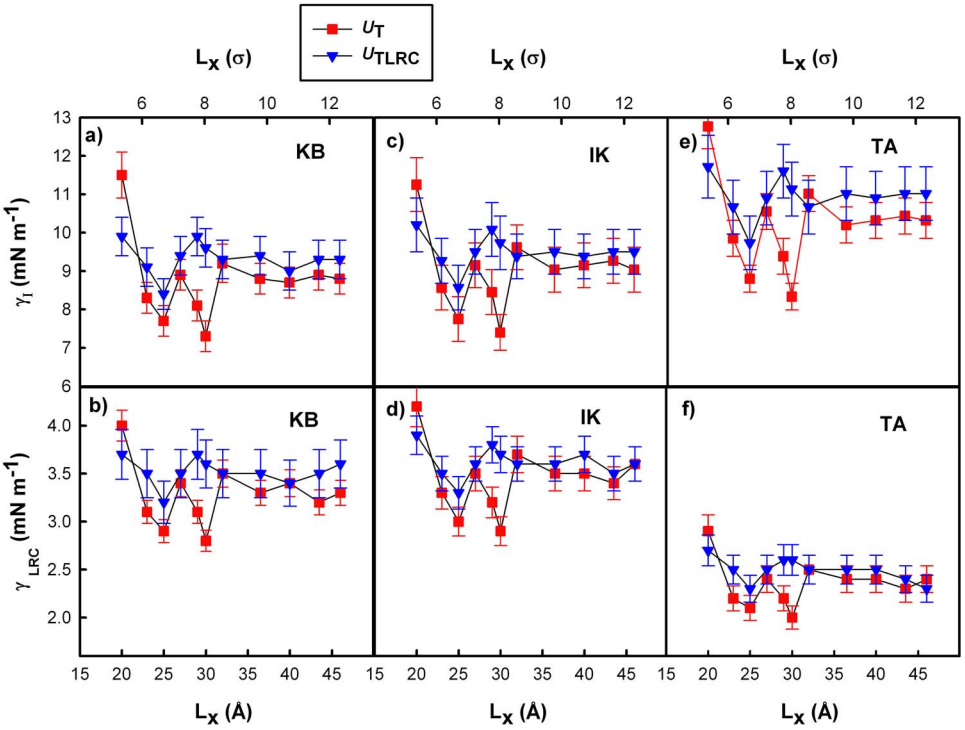

FIG. 2. (Color online) Intrinsic (γ_l) and LRC (γ_{LRC}) contributions to the surface tension as a function of the interfacial area calculated with the KB, IK, and TA approaches from MC simulations carried out with U_{TLRC} (triangle) and U_T (square).

dence of γ with L_z. It corresponds to a ratio (L_z/L_x) slightly larger than 5. All these results show that in order to eliminate all system size effects, the U_{TLRC} potential allows the use of $L_x=L_y=9\sigma$ and $L_z=50\sigma$, whereas the U_T potential requires an interfacial area of $11\times11\sigma^2$ and a box length in the direction normal to the interface of 60σ. These latter box dimensions obtained from MC simulations without LRC contributions are consistent with those recommended by other authors.[4]

The fact that the oscillatory behavior of γ with respect to the interfacial area and to L_z is damped at smaller values of L_x and L_z with U_{TLRC} explains why we did not observe significant finite-size effects on the surface tension in our previous works.[11,39–42] This attractive result shows that the methodology consisting of incorporating the LRC part to the configurational energy on the fly allows to reduce the finite-size effects on the surface tension. As a consequence, this methodology allows the use of smaller box dimensions and number of molecules. This aspect was underlined by Guo and Lu[12] in their original paper. However, they did not demonstrate that the incorporation of the LRC into the computational algorithm allowed to reduce the finite-size effects on the surface tension.

In order to analyze the impact of the system sizes on the different contributions to the surface tension, the total surface tension has been split into intrinsic and LRC parts. These two contributions are represented in Fig. 2 as a function of the interfacial area for KB, IK, and TA. The different parts of the surface tensions were calculated with a cutoff radius of 9.3 Å (2.5σ). With this cutoff, the LRC contribution to the surface tension reaches 30% of the total value for the KB and IK mechanical definitions and 20% for the TA thermodynamic definition. This underlines the importance of the calculation of such LRC contributions and the need of an appropriate combination of the LRC and the intrinsic surface tensions. First, we observe that the oscillatory behavior affects both the intrinsic part and the LRC contribution to the surface tension. We observe that the extrema are located at the same points along the oscillation curves for the intrinsic and LRC contributions. The main previous conclusions remain valid: The use of the LRC to the energy during the MC simulation dampens the oscillations of γ for both the intrinsic and the LRC parts. Similar conclusions can be drawn concerning the dependence of the different parts of the surface tension with the box dimension L_z (results not shown here).

Alejandre and co-workers[1,3,43,47] explained the oscillatory variation in γ with respect to the surface area by the use of both small interfacial areas and periodic boundary conditions. These two factors lead to an artificial stress in the liquid region. These authors have recently shown that this anisotropy in the pressure tensor occurs even in bulk systems[3] in noncubic boxes. The calculation of the anisotropy of the pressure in a heterogeneous system must be done using a local definition of the pressure components. The degree of anisotropy $\Delta\gamma$ could be calculated via the profile of the surface tension $\gamma(z)$ in the liquid phase. $\Delta\gamma$ is thus calculated from the difference of $\gamma(z_2)-\gamma(z_1)$, where z_1 and z_2 are the two limit z-positions defining the bulk liquid region. This quantity measures the difference between the diagonal elements of the pressure tensor along the z-direction. As expected from the mechanical equilibrium in a bulk liquid phase, $p_{xx}=p_{yy}=p_{zz}=p$ and then $\Delta\gamma$ should be equal to zero. Before calculating the degree of anisotropy of the pressure tensor, the difference between the normal and tangential pressure profiles and the corresponding integral $\gamma(z)$ profile is shown for the intrinsic and LRC parts in Fig. 3. Parts (a) and (b) of this figure exhibit these profiles for two L_x values (9.8σ and 12.3σ) with the same L_z (52.5σ) value, whereas

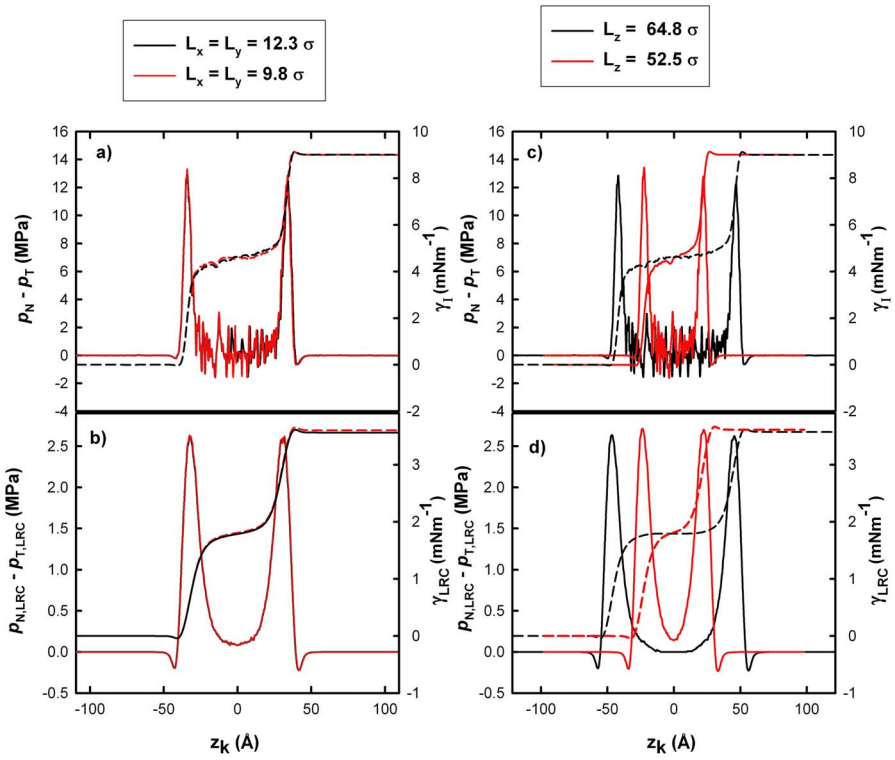

FIG. 3. (Color online) $p_N - p_T$ pressure profiles calculated for (a) two different interfacial areas and (c) two different L_z dimensions; $p_{N,\mathrm{LRC}} - p_{T,\mathrm{LRC}}$ profiles calculated for (b) two different interfacial areas and (d) two different L_z dimensions. The integrals of the $p_N - p_T$ profiles are plotted in the right axis.

parts (c) and (d) present the $p_N - p_T$ profiles for two L_z (52.5σ and 64.8σ) box dimensions with L_x fixed to 12.3σ. The profiles of the pressure components were calculated from the IK definition. First, we do not observe any significant changes on Figs. 3(a) and 3(b) when the interfacial area is increased from $9.8\sigma^2$ to $12.3\sigma^2$. However, these figures reveal that the integrals of the $p_N - p_T$ profiles are definitely not flat in the bulk liquid regions between the two interfaces for the intrinsic and LRC parts. This indicates that the liquid region contributes a little bit to the surface tension. Interestingly, when the L_z dimension is increased up to 64.8σ, the $\gamma(z)$ integral profiles of the intrinsic and the LRC contributions shown in Figs. 3(c) and 3(d) are flatter in the liquid region indicating that a more developed liquid phase contributes much less to the surface tension.

Figure 4(a) shows that the degree of anisotropy $\Delta\gamma$ decreases from 2 to 0.6 mN m^{-1} when the interfacial area changes from $5.4\times5.4\sigma^2$ to $12.3\times12.3\sigma^2$. It corresponds to a decrease in $\Delta\gamma$ from 0.13 to $0.040\sigma^2/\epsilon$ in reduced units. These values of degree of anisotropy are slightly smaller than those calculated by Gonzalez-Melchor *et al.*[3] from bulk LJ fluids in noncubic boxes. These authors found a stress anisotropy close to $0.5\sigma^2/\epsilon$ for interfacial areas slightly larger than $5.5\times5.5\sigma^2$. This corresponds to a value of 7.5 mN m^{-1} for methane at $T=120$ K. More exactly, such values are close to the intrinsic surface tension of methane. On the other hand, we find in the present study that the stress anisotropy $\Delta\gamma$ calculated from the integral of the $p_N - p_T$ profile is rather close in magnitude to the value of the LRC contribution of γ. The way of calculating this property can explain in part this difference in magnitude. It can also be seen in Fig. 4(b) that the increase in the L_z dimension impacts more on the decrease on the stress anisotropy than the increase in L_x. This agrees with the observation done for the

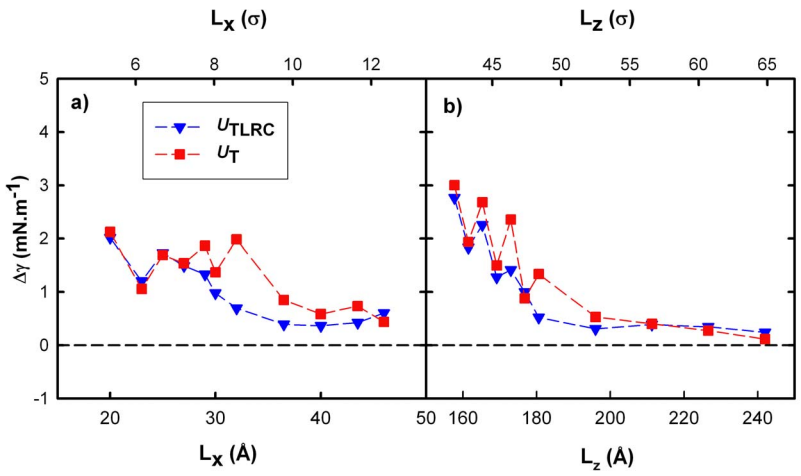

FIG. 4. (Color online) Stress anisotropy $\Delta\gamma$(mN m^{-1}) as a function of (a) L_x and (b) L_z for U_{TLRC} (triangle) and U_T (square) potentials.

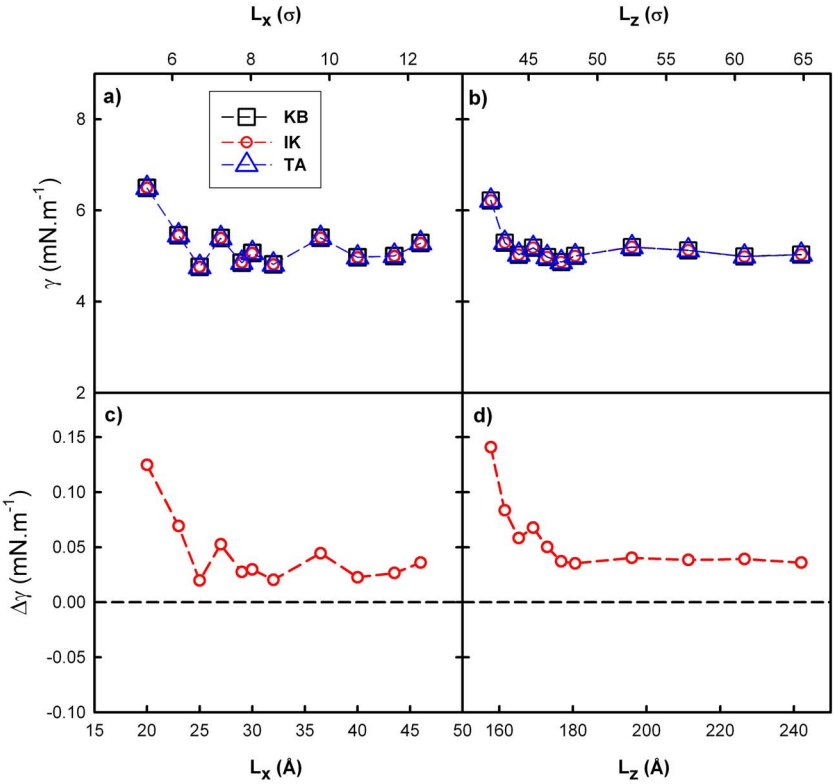

FIG. 5. (Color online) (a) and (b) Surface tension values (mN m^{-1}) calculated as a function of (a) L_x and (b) L_z dimensions for KB, IK, and TA approaches. Stress anisotropy (mN m^{-1}) as a function of (c) L_x and (d) L_z dimensions. All these calculations have been performed using the spline potential U_{SP}. The error bars are smaller than the symbols.

$p_N - p_T$ profiles of Figs. 3(c) and 3(d). Indeed, the stress anisotropy is reduced by a factor of 30 when the L_z dimension changes from 42σ to 65σ. $\Delta\gamma$ is close to 0.1 mN m^{-1} for the largest L_z dimension. From the different curves of Fig. 4, we may claim that there is a relation between the stress anisotropy and the finite-size effects of the surface tension. The ability of the U_{TLRC} potential to reduce the oscillatory effects does result in a slight reduction in the degree of anisotropy. Additionally, it may be surprising at first glance that the surface tension calculated from the TA method also shows an oscillatory variation with respect to the interfacial area because the TA method uses the configurational energy for the calculation of γ. However, within the perturbation formalism, the pressure components can be calculated from performing compression or expansion perturbations.[48] The resulting operational expressions of the pressure show that the pressure can be directly related to the change in the configurational energy due to the perturbation process. It explains why the finite-size effects of the surface tension are also reproduced with the TA approach.

When MC simulations are carried out using a LJ potential changed by the addition of a polynomial function, the variations in the surface tension with respect to L_x and L_z are shown in Figs. 5(a) and 5(b) for the three surface tension calculations. The values of the surface tensions are also listed in Table II. Figures 5(a) and 5(b) and Table II demonstrate that the different IK, KB, and TA approaches give the same values of the surface tension, whereas the use of truncated

TABLE II. Values of surface tension (mN m^{-1}) calculated using the KB, IK, and TA approaches in MC simulations carried out with the LJ potential changed by the addition of a polynomial function. The surface tension is given for various interfacial areas and L_z box dimensions. The subscripts give the accuracy of the last decimal(s), i.e., 6.5_1 means 6.5 ± 0.1.

Constant L_z				Constant $A = L_x L_y$			
$L_x = L_y$ (Å)	γ_{KB}	γ_{IK}	γ_{TA}	L_z (Å)	γ_{KB}	γ_{IK}	γ_{TA}
20.0	6.5_1	6.5_1	6.5_1	157.7	6.2_1	6.2_1	6.2_1
23.0	5.5_1	5.5_1	5.4_1	161.5	5.3_1	5.3_1	5.3_1
25.0	4.8_1	4.8_1	4.8_1	165.3	5.0_1	5.0_1	5.0_1
27.0	5.4_1	5.4_1	5.4_1	169.2	5.2_1	5.2_1	5.2_1
29.0	4.8_1	4.8_1	4.8_1	173.0	5.0_1	5.0_1	5.0_1
30.0	5.1_1	5.1_1	5.1_1	176.8	4.9_1	4.9_1	4.9_1
32.0	4.8_1	4.8_1	4.8_1	180.6	5.0_1	5.0_1	5.0_1
36.5	5.4_1	5.4_1	5.4_1	196.0	5.2_1	5.2_1	5.2_1
40.0	5.0_1	5.0_1	5.0_1	211.3	5.1_1	5.1_1	5.1_1
43.5	5.0_1	5.0_1	5.0_1	226.6	5.0_1	5.0_1	5.0_1
46.0	5.3_1	5.3_1	5.3_1	242.0	5.0_1	5.0_1	5.0_1

TABLE III. Surface tension values (mN m^{-1}) calculated from *NVT* MC simulations using different cutoff distances (r_c). These MC simulations are performed using the U_{TLRC} and the U_T potentials with an interfacial area of 50×50 Å^2 and a L_z dimension of 230 Å. The intrinsic and LRC parts of the surface tensions are given for the KB, IK, and TA definitions. The two last columns correspond to values of surface tension calculated by different methodologies and definitions as indicated in the legend. The subscripts give the accuracy of the last decimal(s), i.e., 12.7_6 means 12.7 ± 0.6.

		γ_{KB}		γ_{IK}		γ_{TA}			
r_c (Å)	$r_c(\sigma)$	γ_{LRC}	γ	γ_{LRC}	γ	γ_{LRC}	γ	γ [a]	γ
					U_{TLRC}				
9.3	2.5	3.5_1	12.7_6	3.5_1	12.5_5	2.4_1	12.4_4	13.4_3	13.4_3 [b]
11.2	3.0	3.2_1	12.4_6	3.2_1	12.4_5	2.2_1	12.2_5	13.2_3	
13.1	3.5	2.8_1	13.2_5	2.8_1	13.0_4	1.9_1	12.9_6	13.1_4	
14.9	4.0	2.4_1	13.0_6	2.3_1	12.8_5	1.7_1	12.6_5		13.5_3 [c]
16.8	4.5	1.9_1	12.3_4	1.9_1	12.0_6	1.3_1	12.0_4		
18.7	5.0	1.5_1	12.7_5	1.5_1	12.6_5	1.0_1	12.4_5		
20.5	5.5	1.1_1	12.8_6	1.0_1	12.6_5	0.8_1	12.5_5		12.7_1 [d]–12.9_2 [e]
22.4	6.0	0.7_1	12.8_5	0.6_1	12.7_4	0.4_1	12.6_5		
					U_T				
9.3	2.5	3.2_1	13.2_6	3.1_1	13.1_5	2.5_1	13.3_6		
11.2	3.0	3.2_1	12.0_4	3.2_1	11.9_5	2.2_1	11.8_4		
13.1	3.5	2.5_1	13.8_5	2.4_1	13.4_6	1.8_1	13.6_5		
14.9	4.0	2.1_1	11.7_4	2.0_1	11.3_5	1.7_1	11.6_5		
16.8	4.5	1.7_1	12.5_5	1.6_1	12.0_4	1.3_1	12.4_6		
18.7	5.0	1.2_1	11.5_4	1.1_1	11.1_5	1.0_1	11.6_4		
20.5	5.5	0.9_1	13.0_5	0.7_1	12.7_6	0.6_1	12.8_5		
22.4	6.0	0.5_1	12.0_5	0.3_1	11.6_6	0.3_1	11.9_5		

[a]From MD simulations where the dispersive energy part is calculated from the lattice sums (Ref. 5).
[b]From MD simulations using the tail correction scheme of Shen (Ref. 13).
[c]From MD simulations using the tail correction scheme of Shen (Ref. 13).
[d]From standard MD simulations (IK method) without any treatment of the LRCs (Ref. 4).
[e]From standard MC simulations (TA method) without any treatment of the LRCs (Ref. 10).

potentials leads to slight differences in the intrinsic part of the surface tension within the different definitions. It means that when discontinuities are removed in the force and energy equations, the definitions using either the energy or the derivative of the energy in their operational expressions are equivalent. It also means that the discontinuities due to the use of truncated potentials are not only the cause of differences between MC and MD simulations but are also responsible for the differences between the values of surface tension calculated from mechanical and thermodynamic routes. The variation in the surface tension with respect to the interfacial area shown in Fig. 5(a) cannot be interpreted in terms of oscillations. From surface areas larger than $6\times6\sigma^2$, the surface tension is almost constant within the error bars. The same observation can be done in Fig. 5(b) for the dependence of the surface tension with respect to the dimension L_z. Parts (c) and (d) of Fig. 5 display the anisotropy stress as a function of box dimensions. Let us recall that the degree of anisotropy is about 20% of the intrinsic part of the surface tension for the smallest interfacial area with the use of truncated potentials. The use of the spline potential reduces the degree of anisotropy to 1.5% of the intrinsic part with the same smallest interfacial area and to 0.5% for the largest studied interfacial areas. The fact that no oscillation of the surface tension with the box dimensions is observed and that the degree of anisotropy is very small for all system sizes reinforces the idea that the finite-size effects of the surface tension are largely due to the anisotropy of the pressure tensor. Nevertheless, the origin of the stress anisotropy cannot be attributed only to small interfacial areas combined with the use of periodic boundary conditions. Indeed, the present study shows that the truncation effects play a major role in the anisotropy of the pressure components, especially when the cutoff radius is not very large (2.5σ).

We complete this work by studying the dependence of the surface tension with respect to the cutoff radius. To do so, we use a relatively large box with $L_x=L_y=50\times50$ Å^2 ($13.4\times13.4\sigma^2$) and $L_z=230$ Å (61.6σ). These box dimensions respect the recommendations given above. The cutoff radius changes from 9.3 to 22.4 Å equivalently from 2.5σ to 6σ. The limit value of 6σ can be considered as enough to approach the full LJ potential.[4] Two types of simulations are carried out: One with the U_{TLRC} potential and another one with the U_T potential. The obtained values for the total surface tension and for the LRC contributions are reported in Table III as a function of r_c for KB, IK, and TA approaches. We also report for comparison the values of surface tensions calculated by other authors with different methodologies. Values of surface tension at $T=120$ K calculated from MD simulations using either the lattice sums for the calculation of the dispersive part of the LJ potential[5] or the tail correction scheme of Shen *et al.*[13] are listed in Table III along with values calculated from MC simulations with the TA method.[10] We observe that the different values of surface tensions agree very well with the standard deviations.

The evolution of these different contributions is represented as a function of the cutoff radius in Fig. 6. As

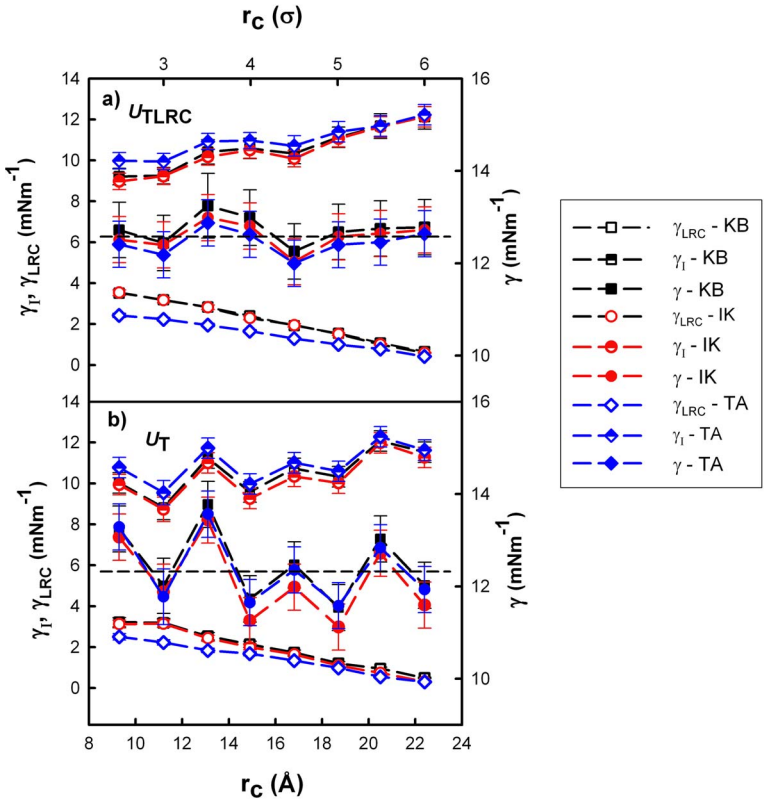

FIG. 6. (Color online) Intrinsic (γ_I) and LRC (γ_{LRC}) contributions to the surface tensions (left axis) and total surface tension (γ) (right axis) as a function of the cutoff radius calculated with (a) the U_{TLRC} potential and (b) the U_T potential. The error bars of the LRC parts of the surface tensions are smaller than the symbols.

expected,[49] the intrinsic part of the surface tension increases with the cutoff radius, whereas the LRC part decreases as the cutoff increases. Parts (a) and (b) of Fig. 6 establish that the decrease in the LRC contributions with r_c is linear for the two truncated potentials. Concerning the intrinsic part, its increase with r_c is more regular for the U_{TLRC} potential. For the U_T potential, the increase in the intrinsic surface tension is subjected to oscillations. This explains the small oscillatory behavior of the total surface tension with r_c when U_T is used. Interestingly, the total surface tension calculated from U_{TLRC} becomes cutoff independent whatever is the definition used. This result agrees very well with the conclusions of Errington and co-workers[13] even if these authors used a different strategy for correcting the configurational energy during the simulation. By using the LRC part of the energy within the Metropolis scheme, it is possible to reduce the box dimensions and the cutoff radius as long as LRCs are appropriately applied to the surface tension at the end of the simulation. We also note that the three definitions give the same surface tension values indicating that the expressions of the LRC contributions are accurately taken into account. The comparison between MC simulations using U_{TLRC} and U_T is instructive: The dependence of the total surface tension with the cutoff is less sensitive to fluctuations than that determined with the U_{TLRC} potential. We do observe a slight decrease in the surface tension with r_c with the U_T potential.

V. CONCLUSIONS

In the introduction of this paper, we have addressed some fundamental points concerning the calculation of liquid-vapor surface tensions of a LJ fluid from a two-phase MC simulation. It was demonstrated by different authors[1,2,43] that the surface tension is subjected to oscillations with respect to the interfacial area. In these works, the surface tension was calculated from the virial route using the KB expression. No LRC contribution was added in the calculation.

In the present work, the dependence of the surface tension with respect to the system sizes has been recovered for mechanical (KB and IK) and thermodynamic (TA) definitions. We have demonstrated that the oscillatory variations affect both the intrinsic and the LRC contributions to the surface tension. In the present study, it has been demonstrated that the use of LRCs to energy in the Metropolis scheme allows to reduce significantly the oscillatory behavior of the surface tension with respect to both the interfacial area and the box dimension in the direction normal to the interface. This strategy of using the LRC contributions to the energy on the fly allows to use smaller interfacial areas. We have also shown that the choice of the L_z box dimension value really impacts on the anisotropy of the pressure tensor. We have found a relationship between the finite-size effects on the surface tension and the anisotropy of the pressure tensor components when truncated potentials were used in the MC simulations.

To study the potential truncation effects on the variations in the surface tension with the box dimensions, we have changed the Lennard potential by the addition of a polynomial function so that both the energy and the force equations are continuous at the cutoff radius. Interestingly, the variations in the surface tension with respect to L_x and L_z do not show any oscillatory behavior and the degree of anisotropy of the pressure components is very small for all the box sizes studied. It supports the idea that the oscillatory behavior of the surface tension can be related to the anisotropy of the

pressure components. However, we have shown that the origin of the anisotropy of the pressure cannot be only attributed to the use of small interfacial areas and periodic boundary conditions. It has been established in this work that the truncation effects can play a significant role in the anisotropy of the pressure.

The dependence of the surface tension with the cutoff radius has been studied for two types of potentials. We have concluded that incorporating the LRCs to the energy into the Metropolis scheme and using appropriate LRC expressions for the different definitions of the surface tension result in obtaining cutoff-independent surface tension values whatever is the route used for the calculation. We have obtained larger fluctuations in the variations in the surface tension with the cutoff when the LRC contributions to the energy are not considered during the course of the simulation. These fluctuations are however in the order of magnitude of the error bars.

ACKNOWLEDGMENTS

The authors would like to acknowledge the support of the French Agence Nationale de la Recherche (ANR) under grant SUSHI (Grant No. ANR-07-BLAN-0268) "SimUlation de Systèmes Hétérogènes et d'Interfaces."

[1] P. Orea, J. Lopez-Lemus, and J. Alejandre, J. Chem. Phys. **123**, 114702 (2005).
[2] J. R. Errington and D. A. Kofke, J. Chem. Phys. **127**, 174709 (2007).
[3] M. Gonzalez-Melchor, P. Orea, J. Lopez-Lemus, F. Bresme, and J. Alejandre, J. Chem. Phys. **122**, 094503 (2005).
[4] A. Trokhymchuk and J. Alejandre, J. Chem. Phys. **111**, 8510 (1999).
[5] J. Lopez-Lemus and J. Alejandre, Mol. Phys. **100**, 2983 (2002).
[6] F. Goujon, P. Malfreyt, A. Boutin, and A. H. Fuchs, J. Chem. Phys. **116**, 8106 (2002).
[7] P. Grosfils and J. F. Lutsko, J. Chem. Phys. **130**, 054703 (2009).
[8] F. Goujon, P. Malfreyt, J. M. Simon, A. Boutin, B. Rousseau, and A. H. Fuchs, J. Chem. Phys. **121**, 12559 (2004).
[9] C. Ibergay, A. Ghoufi, F. Goujon, P. Ungerer, A. Boutin, B. Rousseau, and P. Malfreyt, Phys. Rev. E **75**, 051602 (2007).
[10] G. J. Gloor, G. Jackson, F. J. Blas, and E. de Miguel, J. Chem. Phys. **123**, 134703 (2005).
[11] A. Ghoufi, F. Goujon, V. Lachet, and P. Malfreyt, Phys. Rev. E **77**, 031601 (2008).
[12] M. Guo and B. C. Y. Lu, J. Chem. Phys. **106**, 3688 (1997).
[13] V. K. Shen, R. D. Mountain, and J. R. Errington, J. Phys. Chem. B **111**, 6198 (2007).
[14] J. G. Kirkwood and F. P. Buff, J. Chem. Phys. **17**, 338 (1949).
[15] F. B. Buff, Z. Elektrochem. **56**, 311 (1952).
[16] A. G. MacLellan, Proc. R. Soc. London, Ser. A **213**, 274 (1952).
[17] A. G. McLellan, Proc. R. Soc. London, Ser. A **217**, 92 (1953).
[18] J. S. Rowlinson and B. Widom, *Molecular Theory of Capillarity* (Clarendon, Oxford, 1982).
[19] J. H. Irving and J. G. Kirkwood, J. Chem. Phys. **18**, 817 (1950).
[20] J. P. R. B. Walton, D. J. Tildesley, J. S. Rowlinson, and J. R. Henderson, Mol. Phys. **48**, 1357 (1983).
[21] J. P. R. B. Walton and K. E. Gubbins, Mol. Phys. **55**, 679 (1985).
[22] E. Salomons and M. Mareschal, J. Phys.: Condens. Matter **3**, 3645 (1991).
[23] E. M. Blokhuis, D. Bedeaux, C. D. Holcomb, and J. A. Zollweg, Mol. Phys. **85**, 665 (1995).
[24] J. Alejandre, D. J. Tildesley, and G. A. Chapela, J. Chem. Phys. **102**, 4574 (1995).
[25] M. Mecke and J. Winkelmann, J. Chem. Phys. **107**, 9264 (1997).
[26] M. Mecke, J. Winkelmann, and J. Fischer, J. Chem. Phys. **110**, 1188 (1999).
[27] J. Janecek, J. Phys. Chem. B **110**, 6264 (2006).
[28] J. R. Errington, Phys. Rev. E **67**, 012102 (2003).
[29] J. R. Errington, J. Chem. Phys. **118**, 9915 (2003).
[30] K. Binder, Phys. Rev. A **25**, 1699 (1982).
[31] J. J. Potoff and A. Z. Panagiotopoulos, J. Chem. Phys. **112**, 6411 (2000).
[32] J. K. Singh, D. A. Kofke, and J. R. Errington, J. Chem. Phys. **119**, 3405 (2003).
[33] J. K. Singh and J. R. Errington, J. Phys. Chem. B **110**, 1369 (2006).
[34] E. M. Grzelak and J. R. Errington, J. Chem. Phys. **128**, 014710 (2008).
[35] A. M. Ferrenberg and R. H. Swendsen, Phys. Rev. Lett. **61**, 2635 (1988).
[36] A. M. Ferrenberg and R. H. Swendsen, Phys. Rev. Lett. **63**, 1195 (1989).
[37] V. K. Shen and J. R. Errington, J. Chem. Phys. **124**, 024721 (2006).
[38] J. Janecek, H. Krienke, and G. Schmeer, J. Phys. Chem. B **110**, 6916 (2006).
[39] A. Ghoufi, F. Goujon, V. Lachet, and P. Malfreyt, J. Chem. Phys. **128**, 154716 (2008).
[40] A. Ghoufi, F. Goujon, V. Lachet, and P. Malfreyt, J. Chem. Phys. **128**, 154718 (2008).
[41] F. Biscay, A. Ghoufi, F. Goujon, V. Lachet, and P. Malfreyt, J. Phys. Chem. B **112**, 13885 (2008).
[42] F. Biscay, A. Ghoufi, V. Lachet, and P. Malfreyt, "Calculation of the surface tension of cyclic and aromatic hydrocarbons from Monte Carlo simulations using an Anisotropic United Atom model (AUA)," Phys. Chem. Chem. Phys. (2009) (in press).
[43] M. Gonzalez-Melchor, F. Bresme, and J. Alejandre, J. Chem. Phys. **122**, 104710 (2005).
[44] D. Möller and J. Oprzynski, Mol. Phys. **75**, 363 (1992).
[45] A. Ghoufi and P. Malfreyt, Mol. Phys. **104**, 2929 (2006).
[46] A. J. C. Ladd and L. V. Woodcok, Mol. Phys. **36**, 611 (1978).
[47] M. E. Velazquez, A. Gama-Goicochea, M. Gonalez-Melchor, M. Neria, and J. Alejandre, J. Chem. Phys. **124**, 084104 (2006).
[48] E. de Miguel and G. Jackson, J. Chem. Phys. **125**, 164109 (2006).
[49] F. J. Blas, L. G. MacDowell, E. de Miguel, and G. Jackson, J. Chem. Phys. **129**, 144703 (2008).